Electronic Supplementary Material (ESI) for ChemComm.

Supporting Information

Optimizing phenyl selenide-based BODIPYs as fluorescent probes for diagnosing cancer and drug-induced liver injury via cysteine

Xiaoyan Lu,‡[a] Nannan Wang,‡[a] Yuanfang Tao,‡[a] Jiamin Wang,*[c] Xin Ji,[b] Jinying Liu,[a] Weili Zhao,*[ab] and Jian Zhang*[a]

[a] Key Laboratory for Special Functional Materials of Ministry of Education, School of Materials Science and Engineering, Henan University, Kaifeng, 475004, P. R. China.
[b] School of Pharmacy, Institutes of Integrative Medicine, Fudan University, Shanghai, 201203, P. R. China.
[c] Key Laboratory of Natural Medicine and Immuno-Engineering of Henan Province, Henan University, Kaifeng 475004, China.
E-mail:
jmwang@henu.edu.cn; zhaoweili@fudan.edu.cn; jianzhang@henu.edu.cn

Table of contents

1. Materials and General Experimental Methods

1.1 Materials and instruments

In Chemical reagents were ordered from commercial suppliers and used as received. In all experiments enantiomerically pure natural amino acids were used except for Hcy which was used as the racemate. Organic solvents were used after purification by standard methods. Chromatographic grade of acetonitrile and deionized water were utilized in the detection. ^{1}H NMR spectra were taken from Varian Model Mercury 400 MHz spectrometer. ^{1}H NMR data of chemical shifts (δ) were given in ppm (s = singlet, d = doublet, t = triplet, q = quartet, m = multiplet) using $CDCl_3$ (δ= 7.26 ppm) and dimethyl sulfoxide (δ = 2.5 ppm) as reference. ^{13}C NMR spectra were recorded on Varian Model Mercury 100 MHz spectrometer and the chemical shifts (δ) were reported in ppm with $CDCl_3$ and d_6-DMSO at δ 77.0 and 39.4 ppm as internal standard. Mass spectra were obtained with AB SCIEX MALDI-TOF/TOF 5800 mass spectrometer. Ultraviolet-visible (UV-vis) spectroscopic studies were performed on Perkin-Elmer Model Lambda 950 UV/vis spectrophotometer. Fluorescence spectra were measured on FluoroSENS spectrophotometer. The cell imaging was recorded with an inverted fluorescence microscope (DMI8). Whole body imaging experiments were performed using a small animal real-time *in vivo* fluorescence imaging system (VISQUE In Vivo Smart).

1.2 General procedure for fluorescence measurement

Determination of the detection limit. The detection limit was calculated based on the fluorescence titration. In the absence of Cys, the fluorescence emission spectrum of **BDP-Se-MOP and BDP-Se-MOS** were measured by five times and the standard deviation of blank measurement was achieved. To gain the slop, the fluorescence intensity at 545 nm /613 nm were plotted to the concentration of Cys/Hcy. So the detection limit was calculated with the following equation:

Detection limit = 3σ/k

Where σ is the standard deviation of blank measurement, k is the slop between the fluorescence intensity versus Cys concentration.

Procedure for Cys and Hcy/GSH Sensing. A stock solution of **BDP-Se-M** (1 mM) was prepared in 100% CH_3CN and was subsequently diluted to prepare appropriate concentration solutions of **BDP-Se-M** in CH_3CN/PBS buffer (pH 7.4, 30% CH_3CN in 10 mM PBS). Cys/Hcy/GSH stock solutions were freshly prepared prior to each experiment. For the calibration curve, solutions of **BDP-Se-M** were incubated with different concentrations of Cys and Hcy/GSH at 37°C for 3 min and 5 min respectively, and spectral data were recorded. Excitation was at 365 nm and emission was detected at 494 nm for Cys. Excitation was at 456 nm and emission was detected at 540 nm for Hcy/GSH.

Procedure for Cys/Hcy Sensing. A stock solution of **BDP-Se-MOP** (1 mM) was prepared in 100% CH_3CN and was subsequently diluted to prepare appropriate concentration solutions of **BDP-Se-MOP** in CH_3CN/PBS buffer (pH 7.4, 40% CH_3CN in 10 mM PBS). **Cys/Hcy** stock solutions were freshly prepared prior to each experiment. For the calibration curve, solutions of **BDP-Se-MOP** were incubated with different concentrations of Cys/Hcy at 37°C for 2 min and 45 min respectively, and spectral data were recorded. Excitation was at 456 nm and emission was detected at 545 nm.

Procedure for Cys Sensing. A stock solution of **BDP-Se-MOS** (1 mM) was prepared in 100% DMSO and was subsequently diluted to prepare appropriate concentration solutions of **BDP-Se-MOS** in CH_3CN/PBS buffer (pH 7.4, 50% CH_3CN in 10 mM PBS). Cys stock solutions were freshly prepared prior to each experiment. For the calibration curve, solutions of **BDP-Se-MOS** were incubated with different concentrations of Cys at 37°C for 10 min, and spectral data were recorded. Excitation was at 525 nm and emission was detected at 613 nm.

1.3 Cell incubation and fluorescence imaging

Human hepatocellular carcinomas (HepG2), human normal hepatocytes (QSC-7701), human hepatoma cells (SMMC-7721) and mouse mononuclear macrophage leukemia cells (RAW264.7) were all expressed in 10% fetal bovine serum (FBS) and 1% penicillin-streptomycin in high glucose Dulbecco's Modified Eagle Medium (DMEM) in a humidified incubator with 5% CO_2 and 95% air at 37°C.

MTT assay experiment. 3-(4,5-dimethylthiazol-2-yl)-2,5-diphenyltetrazolium bromide (MTT) experiment was performed in 96-well plate to assess the cytotoxicity of **BDP-Se-MOS**. HepG2 cells and QSG-7701 cells were cultured in 96-well plate at a density of 5×10^3 cells/well and incubated for 24 h prior to experimental treatments. The probe **BDP-Se-MOS** was dissolved into the mother stock solution with organic solvent DMSO and medium (1:9), and then diluted to different concentrations (2, 5, 10, 20 and 30 μM) by the medium, so that the content of the organic solvent reaches the acceptable range of cells. Then, **BDP-Se-MOS** in various concentrations (2, 5, 10, 20 and 30 μM) was added to the well and incubated for 24 h. MTT solution (1 mg/mL) was added to each well and continuously incubated for 4 h at 37 °C. Subsequently, MTT solution was removed and DMSO (100 μL/well) was added to each well to dissolve the dark blue formazan crystals. The absorbance was measured at 570 nm by a microplate reader. Cell viability was expressed as a percentage of MTT reduction with the untreated cells as 100%.

Inverted fluorescence microscopy images. All the experiments were conducted in live cells. The probe **BDP-Se-MOS** was dissolved into 1 mM mother liquor with the organic solvent DMSO, and then diluted with culture medium to the incubation concentration so that the content of the organic solvent was less than 1%, ensuring the normal survival of the cells. The microscopic imaging uses Leica DMI8 inverted fluorescence microscope. λ_{ex} = 530-570 nm, λ_{em} = 575-640 nm.

Exogenous or endogenous Cys imaging experiments in live cells. The HepG2 cells were divided into five groups. The first group were incubated with probe **BDP-Se-MOS** (10 μM) for 2 h. The second group were pretreated with NEM (1 mM) for 1

h, and then treated with **BDP-Se-MOS** (10 μM) for 2 h. The third through fifth groups were pretreated with NEM (1 mM) for 1 h, and then treated with Cys/Hcy/GSH (200 μM) for 1 h, respectively. And the probe **BDP-Se-MOS** (10 μM, 2 h) were incubated. The cells were treated with Hoechst 33342 (1 μg/mL) for 10 min. Fluorescence imaging was carried out after washing the cells with PBS for three times.

HepG2 cells, QSC-7701 cells, SMMC-7721 cells and RAW264.7 cells were incubated with **BDP-Se-MOS** (10 μM) for 2 h and Hoechst 33342 (1 μg/mL) for 10 min, and then washed with PBS for three times, which could distinguish between normal cells and cancer cells.

APAP-induced hepatotoxicity in live cells. The HepG2 cells were divided into three groups. The first group were incubated with probe **BDP-Se-MOS** (10 μM) for 2 h. The second group were pretreated with APAP (500 μM) for 8 h. The third group were pretreated with APAP (500 μM, 8 h), and then incubated with NAC (500 μM, 1 h). Two groups were treated with **BDP-Se-MOS** (10 μM, 2 h) and Hoechst 33342 (1 μg/mL) for 10 min. Inverted microscope imaging was carried out after washing the cells with PBS for three times.

1.4 Fluorescence imaging in mice and zebrafish

Adult wild-type zebrafish were provided by the Institute of Brain Research and Rehabilitation, South China Normal University (Guangzhou, China). Adult fish were reared in charcoal-filtered water at 28°C under semi-static conditions with a light-dark photoperiod of 14:10. All fluorescence images were acquired on a stereo microscope under a confocal laser scanning microscope with an excitation wavelength of 530–570 nm and a collection window of 575–640 nm. C57BL/6J mice and Kunming mice were 6-week-old males and were bred in the Experimental Animal Center of Henan University. All animal care and experimental protocols for this study were performed according to the guidelines by the Animal Experiment Ethics Committee of Henan University. All operations were approved by the Animal Experiment Ethics Committee of Henan University (Reference number: HUSOM2017-167). The probe uses 1%

DMSO and castor oil to prepare the mother liquor of corresponding concentration.

Endogenous or exogenous Cys imaging in zebrafish. For bioimaging *in vivo*, adult wild-type zebrafish were divided into three groups. The first group were pretreated with probe **BDP-Se-MOS** (10 μM) for 1 h. The second group and the third group were respectively pretreated with NEM (1 mM) for 30 min, and then treated with **BDP-Se-MOS** (10 μM) for 1 h. Then third group of zebrafish were treated with 200 μM Cys for 30 min. Finally, fluorescence imaging was carried out after the zebrafish were washed three times.

Endogenous or exogenous Cys imaging experiments in mice. The mice were divided into four groups. The first group was injected subcutaneously with PBS (100 μL) for 1 h, and the second group received a subcutaneous injection of **BDP-Se-MOS** (200 μM, 100 μL) were pretreated with NEM (500 μM) for 30 min, and then treated with **BDP-Se-MOS** (200 μM, 100 μL) for 1 h. The fourth group were injected subcutaneously with 500 μM NEM for 30 min, then 100 μM Cys was added for 30 min and finally **BDP-Se-MOS** (200 μM, 100 μL) was incubated for 1 h. The live imaging was monitored using the fluorescence imaging system (VISQUE In Vivo Elite).

Real-time imaging of Cys in mice. The mice were given subcutaneous injection of **BDP-Se-MOS** (200 μM, 100 μL) on the right while an equal amount of normal saline was injected subcutaneously on the left. After incubation, images were taken at time 1, 5, 10, 15, 20, 25, 30, 35, 40 and 60 min, respectively.

Tumor-bearing mouse model. The LLC cells were isolated from the cell culture plate, and about 5×10^6 cells were subcutaneously injected into C57BL/6J mice. Two weeks later, **BDP-Se-MOS** (200 μM, 100 μL) was injected into tumor-bearing mice. The photographs were acquired at different times (0 min, 5 min, 10 min, 20 min, 30 min, 40 min, 50 min, 60 min) by the fluorescence imaging system (VISQUE In Vivo Elite). Moreover, the bio-imaging *via* tail vein injection of **BDP-Se-MOS** (1mg/kg), fluorescence images at different times (0, 1, 6, 12, 24 and 48 h) of tumor mice were harvested after injection.

***In vivo* distribution and clearance experiments of BDP-Se-MOS in mice.** The Kunming mice were given tail vein injection of **BDP-Se-MOS** at a dose of 1 mg/kg.

The control group was tail vein injected with the same amount of saline. After dissecting mice at different times (1, 6, 12, 24 and 48 h), the major organs were placed together and placed in an imaging chamber for fluorescence imaging by a small animal optical intravital imaging system (VISQUE In Vivo Elite).

APAP-induced hepatotoxicity. The first group was intraperitoneally injected with **BDP-Se-MOS** (200 μM, 100 μL) for 1 h. The second group was intraperitoneally injected with APAP (300 mg/kg) for 12 h; the third group was intraperitoneally injected with NAC (300 mg/kg, 30 min) and APAP (300 mg/kg) for 12 h; then the two groups were intraperitoneally injected with **BDP-Se-MOS** (200 μM, 100 μL) for 1 h. The control group was intraperitoneally injected with the same amount of PBS. After dissecting all these Kunming mice, the major organs were placed together and placed in an imaging chamber for fluorescence imaging by a small animal optical intravital imaging system (VISQUE In Vivo Elite).

2. Synthesis and Characterization

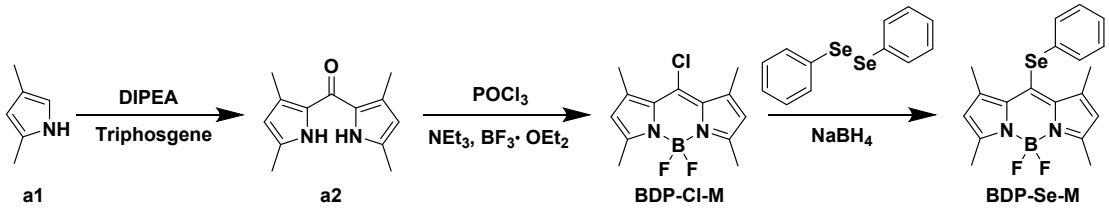

Scheme S1. Synthesis of probe **BDP-Se-M**

Procedure for BDP-Se-M. Compound **BDP-Cl-M** was synthesized according to the synthesis method in the literature.[1] Under nitrogen protection, diphenyl diselenide (50 mg, 0.178 mmol) was dissolved in THF, $NaBH_4$ (13.39 mg, 0.354 mmol) was added at 0°C, and the reduction reaction mixture was stirred for 10 minutes, then the reduced solution was slowly dropped into THF solution containing NEt_3 (0.5 mL) and compound **BDP-Cl-M** (50 mg, 0.354 mmol). The reaction mixture was continued in ice water bath for 20 min. The crude product was obtained by vacuum distillation. Then, purified by silica gel column chromatograph (eluent ratio: PE/DCM, 3: 1, v/v) to yield the target product probe **BDP-Se-M** (orange-red solid, 32 mg, 23%). ^{1}H NMR (400 MHz, $CDCl_3$): δ7.28-7.14 (m, 5H), 6.06 (s, 2H), 2.54 (s, 6H), 2.42 (s, 6H). ^{13}C NMR (100 MHz, $CDCl_3$) δ 155.98, 145.36, 135.00, 133.10, 130.89, 129.83, 128.44, 126.56, 122.77, 17.97, 14.81, 14.78, 14.76. HRMS (Maldi) m/z $[M+H]^+$ calcd for $C_{19}H_{20}BF_2N_2Se^+$: 405.0851; Found: 405.0859.

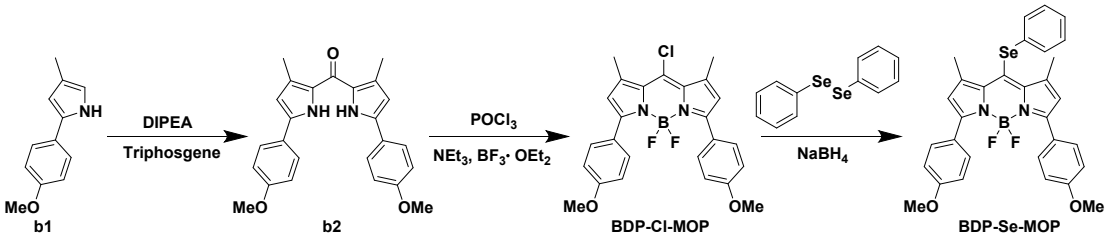

Scheme S2. Synthesis of probe **BDP-Se-MOP**

Procedure for BDP-Se-MOP. Compound **BDP-Cl-MOP** was synthesized according to the synthesis method in the literature.[2] Under nitrogen protection, diphenyl diselenide (74 mg, 0.24 mmol) was dissolved in THF, $NaBH_4$ (15.8 mg, 0.42 mmol) was added at 0°C, and the reduction reaction mixture was stirred for 10 minutes, then

the reduced solution was slowly dropped into THF solution containing NEt_3 (1 mL) and compound **BDP-Cl-MOP** (200 mg, 0.24 mmol). The reaction mixture was continued in ice water bath for 20 min. The crude product was obtained by vacuum distillation. Then, purified by silica gel column chromatograph (eluent ratio: PE/DCM, 1: 1, v/v) to yield the target product probe **BDP-Se-MOP** (mazarine solid, 28 mg, 19%). ^{1}H NMR (400 MHz, $CDCl_3$): δ7.78 (d, J = 8.7 Hz, 2H), 7.35 (d, J = 7.5 Hz, 2H), 7.20 (t, J = 7.3 Hz, 1H), 6.91 (d, J = 7.5 Hz, 2H), 6.37 (s, 2H), 3.82 (s, 6H), 2.52 (s, 6H). ^{13}C NMR (100 MHz, $CDCl_3$) δ 160.67, 156.15, 144.52, 136.59, 133.63, 132.02, 131.10, 131.06, 131.02, 129.91, 128.57, 126.65, 125.10, 123.85, 113.65, 55.27, 18.33. HRMS (Maldi) m/z $[M+H]^+$ calcd for $C_{31}H_{28}BF_2N_2O_2Se^+$: 589.1378; Found: 589.1377.

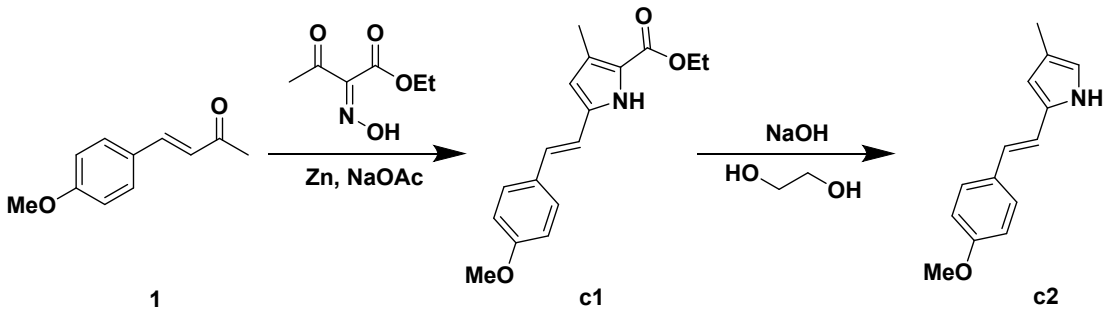

Scheme S3. Synthesis of **c2**

Procedure for Compound c2. In a 1000 mL flask, compound **1** (1.76 g, 11 mmol) and sodium acetate (5.4 g, 66 mmol) were dissolved in propionic acid (30 mL). When the mixture was heated to 150°C, a solution of ethyl-2-(hydroxyimino)-3-oxobutanoate (1.75 g, 11 mmol) in 200 mL propionic acid and zinc dust (7.1 g, 11 mmol) were slowly added to the stirred mixture. After the addition, the mixture was stirred at 150°C for 2 h and cooled to about 70°C. It was then poured into ice/water mixture and allowed to stand overnight. The precipitate was filtered and washed with water until the pH value of filtrate was 7.0. The residue was then recrystallized from ethanol several times to give compound **c2** (28% yield) as a white solid. ^{1}H NMR (400 MHz, d_6-DMSO) δ 10.70 (s, 1H), 7.35 (d, J = 8.4 Hz, 2H), 6.89 (d, J = 8.6 Hz, 2H), 6.76 (q, J = 16.5 Hz, 2H), 6.54 (s, 1H), 6.02 (s, 1H), 3.75 (s, 3H), 2.01 (s, 3H). ^{13}C NMR (100 MHz, d_6-DMSO) δ 158.57, 131.01, 130.94, 127.05, 122.08, 118.68, 118.27, 117.66, 114.66, 110.07, 55.55, 12.32.

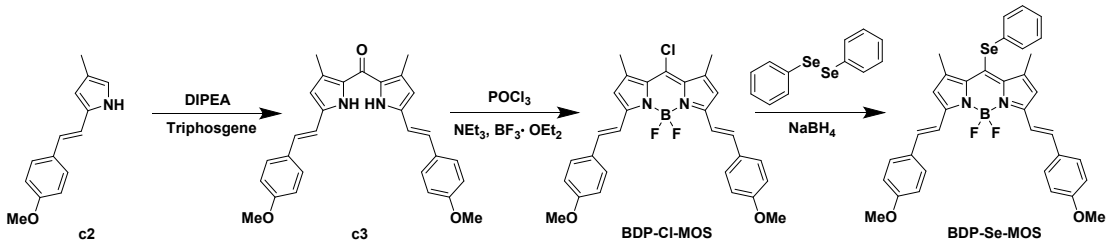

Scheme S4. Synthesis of probe **BDP-Se-MOS**

Procedure for Compound BDP-Cl-MOS. A solution of triphosgene (730 mg, 3.0 mmol) in THF (30 mL) was added to a stirred solution of compound **c2** (800 mg, 3.75 mmol) and DIPEA (1.0 mL, 3.0 mmol) in THF (10 mL) over 30 min at 0°C under nitrogen. The reaction mixture was treated with saturated NaCl solution and the resulting solution was extracted with ethyl acetate. The yellow product (compound **c3**) was obtained by spin drying and directly used in the next step synthesis.

Compound **c3** (425 mg, 0.95mmol) was dissolved in 1,2-dichloroethane (10 mL). Phosphorus oxychloride (50 uL, 0.50 mmol) was added at 0°C under nitrogen, and the mixture gradually warmed to room temperature and stirred for 12 h. Triethylamine (0.8 mL, 6.0 mmol) was added, and the reaction was stirred at 0°C for 5 min. Boron trifluoride etherate (1.1 mL, 7.7 mmol) was added dropwise while maintaining the temperature at 0°C. The mixture gradually warmed to room temperature and stirred for 30 min. The resulting solution was poured out in diethyl ether (300 mL) and extracted with water. After drying over Na_2SO_4, filtration, and evaporation, the crude product was purified by silica gel column chromatography (CH_2Cl_2/PE, 3 : 1, v/v) to yield solid **BDP-Cl-MOS** (150 mg, 30%).^{1}H NMR (400 MHz, $CDCl_3$) δ 7.60 – 7.49 (m, 7H), 7.22 (s, 1H), 6.93 (d, J = 8.6 Hz, 4H), 6.71 (s, 2H), 3.85 (s, 6H), 2.52 (s, 6H). ^{13}C NMR (100 MHz, $CDCl_3$) δ 160.58, 152.48, 141.39, 136.56, 129.43, 129.14, 117.87, 116.87, 114.32, 55.40, 16.90.

Procedure for BDP-Se-MOS. Under nitrogen protection, diphenyl diselenide (75.45 mg, 0.15 mmol) was dissolved in THF, $NaBH_4$ (11 mg, 0.29 mmol) was added at 0°C, and the mixture was stirred for 10 minutes, then the reduced solution was slowly dropped into THF solution containing NEt_3 (0.6 mL) and **BDP-Cl-MOS** (150 mg, 0.29 mmol). The reaction mixture was continued in ice water bath for 20 min. The crude product was obtained by vacuum distillation. Then, purified by silica gel column

chromatograph (eluent ratio: PE/DCM, 4: 1, v/v) to yield the target product probe **BDP-Se-MOS** (green solid, 30 mg, 17%). ^{1}H NMR (400 MHz, $CDCl_3$): δ 7.62 (s, 1H), 7.59 (d, J = 8.6 Hz, 5H), 7.29 (d, J = 7.5 Hz, 3H), 7.23 (s, 3H), 7.18 (d, J = 7.0 Hz, 1H), 6.94 (d, J = 8.7 Hz, 14H), 6.71(s, 2H), 3.86 (s, 6H), 2.50 (s, 6H). ^{13}C NMR (100 MHz, $CDCl_3$) δ 160.61, 152.70, 143.72, 136.78, 133.81, 129.82, 129.57, 129.22, 128.22, 126.38, 119.07, 117.18, 114.34, 55.40, 18.20. HRMS (Maldi) m/z $[M+H]^+$ calcd for $C_{35}H_{31}BF_2N_2O_2Se^+$: 641.1693; Found: 641.1692.

3. Spectral data

Table S1 Bond length and bond order of C-Se obtained from DFT calculations.

Probe	Bond length$_{C\text{-}Se}$/Å	Bond order$_{C\text{-}Se}$
BDP-Se-M	1.89643	0.6199
BDP-Se-MOP	1.89564	0.6277
BDP-Se-MOS	1.89549	0.6326

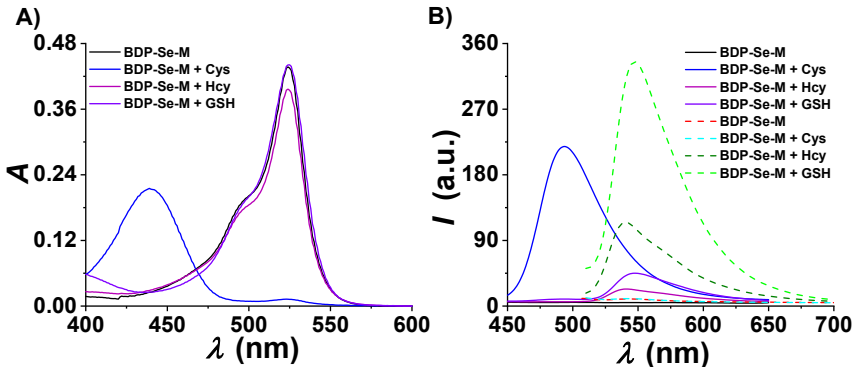

Fig. S1 (A) Absorption and (B) emission spectra of **BDP-Se-M** (10 μM) in the absence and presence of Cys, Hcy, or GSH (100 μM) (solid lines, λ_{ex} = 365 nm; dashed lines, λ_{ex} = 465 nm). Conditions: PBS buffer solutions (pH 7.4, 10 mM, containing 30% CH_3CN), 37°C.

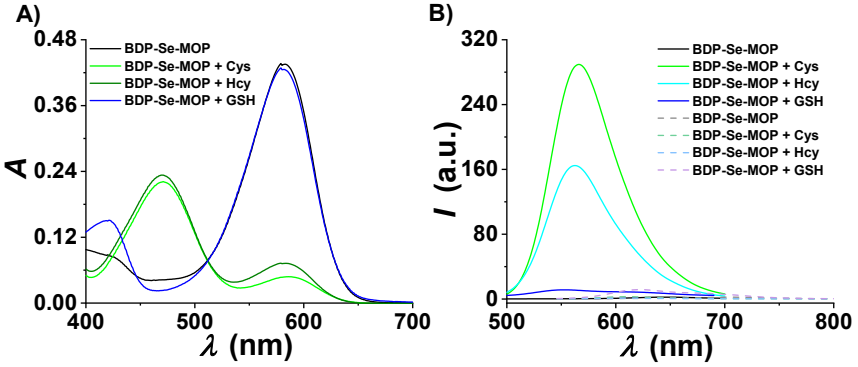

Fig. S2 (A) Absorption and (B) emission spectra of **BDP-Se-MOP** (10 μM) in the absence and presence of Cys, Hcy, or GSH (100 μM) (solid lines, λ_{ex} = 465 nm; dashed lines, λ_{ex} = 525 nm). Conditions: PBS buffer solutions (pH 7.4, 10 mM, containing 40% CH_3CN), 37°C.

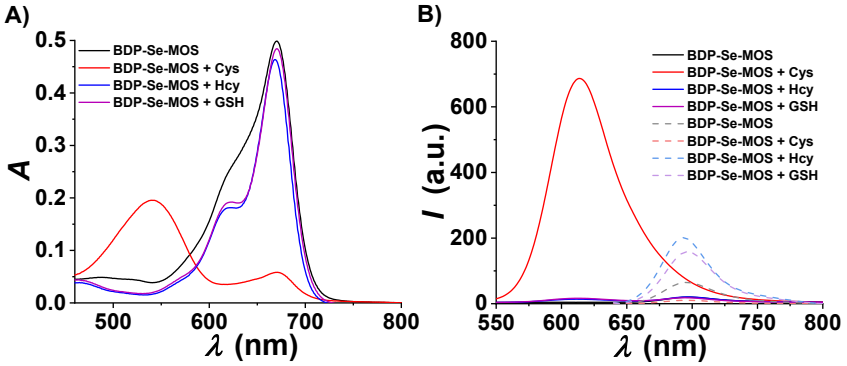

Fig. S3 (A) Absorption and (B) emission spectra of **BDP-Se-MOS** (10 μM) in the absence and presence of Cys, Hcy, or GSH (100 μM) (solid lines, λ_{ex} = 525 nm; dashed lines, λ_{ex} = 613 nm). Conditions: PBS buffer solutions (pH 7.4, 10 mM, containing 50% CH_3CN), 37°C.

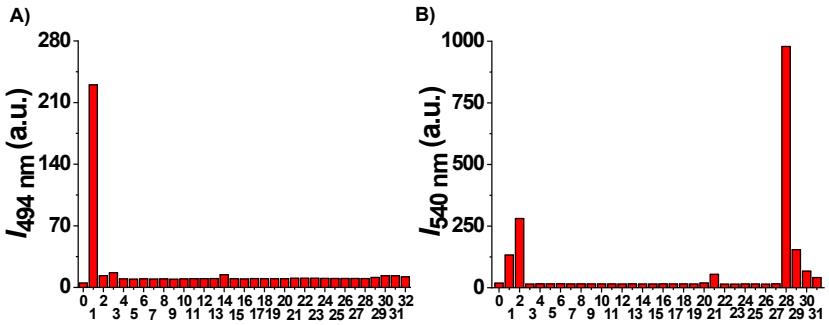

Fig. S4 Fluorescence emission changes of **BDP-Se-M** (10 μM) to various analytes (100 μM) at 37°C. 0. Blank; 1. Cys; 2. Hcy; 3. GSH; 4. Ala; 5. Gln; 6. Ile; 7. Met; 8. Arg; 9. His; 10. Tyr; 11. Asp; 12. Glu; 13. Leu; 14. Gly; 15. Phe; 16. Lys; 17. Thr; 18. Ser; 19. Pro; 20. Try; 21. SO_3^{2-}; 22. $S_2O_3^{2-}$; 23. $S_2O_4^{2-}$; 24. $S_2O_5^{2-}$; 25. HSO_3^-; 26. HS^-; 27. NO·; 28. TBHP; 29. HOCl; 30. H_2O_2; 31. $^1O_2$; 32. $ONOO^-$. (A) λ_{ex} = 365 nm and λ_{em} = 494 nm. (B) λ_{ex} = 456 nm and λ_{em} = 540 nm.

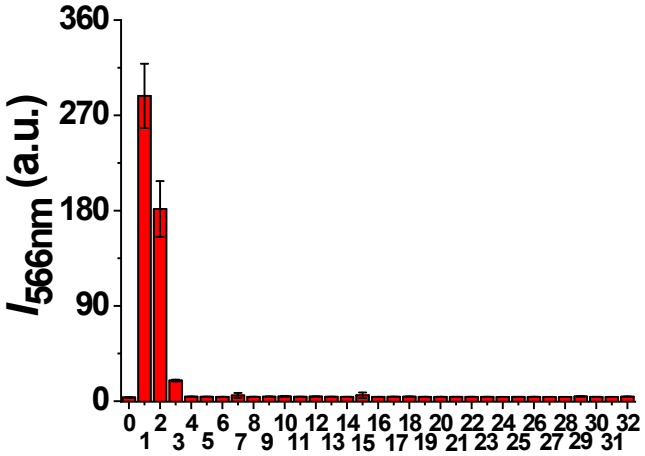

Fig. S5 Fluorescence emission changes of **BDP-Se-MOP** (10 μM) to various analytes (100 μM) at 37°C. 0. Blank; 1. Cys; 2. Hcy; 3. GSH; 4. Ala; 5. Gln; 6. Ile; 7. Met; 8. Arg; 9. His; 10. Tyr; 11. Asp; 12. Glu; 13. Leu; 14. Gly; 15. Phe; 16. Lys; 17. Thr; 18. Ser; 19. Pro; 20. Try; 21. SO_3^{2-}; 22. $S_2O_3^{2-}$; 23. $S_2O_4^{2-}$; 24. $S_2O_5^{2-}$; 25. HSO_3^-; 26. HS^-; 27. NO·; 28. TBHP; 29. HOCl; 30. H_2O_2; 31. $^1O_2$; 32. $ONOO^-$. λ_{ex} = 456 nm and λ_{em} = 566 nm.

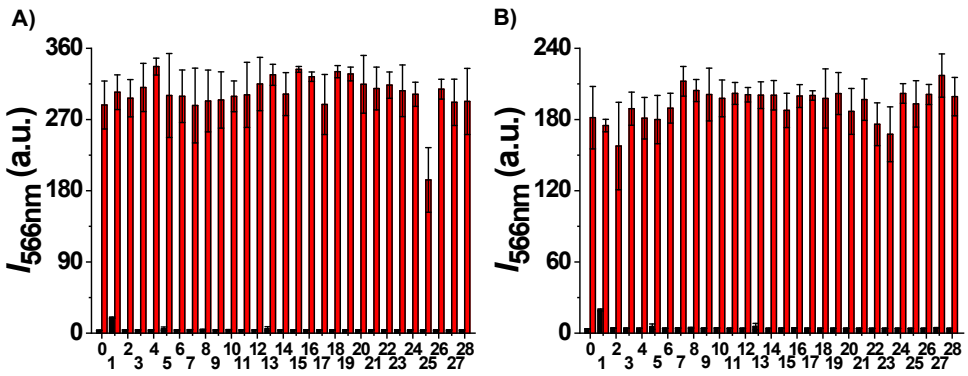

Fig. S6 (A) The **BDP-Se-MOP** (10 μM) fluorescence intensity changes (black bars) of individual analytes (100 μM) in comparison with those (red bars) after addition of Cys (100 μM) at 566 nm. 0. Blank; 1. Hcy; 2. Ala; 3. Gln; 4. Ile; 5. Met; 6. Arg; 7. His; 8. Tyr; 9. Asp; 10. Glu; 11. Leu; 12. Gly; 13. Phe; 14. Lys; 15. Thr; 16. Ser; 17. Pro; 18. Try; 19. SO_3^{2-}; 20. $S_2O_3^{2-}$; 21. $S_2O_4^{2-}$; 22. $S_2O_5^{2-}$; 23. HSO_3^-; 24. HS^-; 25. NO·; 26. TBHP; 27. H_2O_2; 28. $^1O_2$. (B) The **BDP-Se-MOP** (10 μM) fluorescence intensity changes (black bars) of individual analytes (100 μM) in comparison with those (red bars) after addition of Hcy (100 μM) at 566 nm. 0. Blank; 1. GSH; 2. Ala; 3. Gln; 4. Ile; 5. Met; 6. Arg; 7. His; 8. Tyr; 9. Asp; 10. Glu; 11. Leu; 12. Gly; 13. Phe; 14. Lys; 15. Thr; 16. Ser; 17. Pro; 18. Try; 19. SO_3^{2-}; 20. $S_2O_3^{2-}$; 21. $S_2O_4^{2-}$; 22. $S_2O_5^{2-}$; 23. HSO_3^-; 24. HS^-; 25. NO·; 26. TBHP; 27. H_2O_2; 28. $^1O_2$.

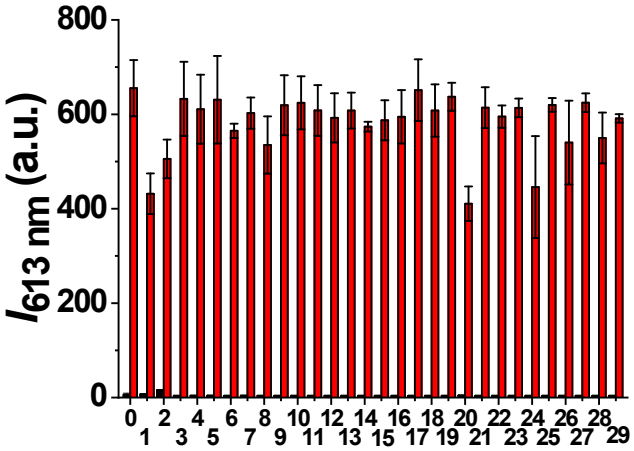

Fig. S7 The **BDP-Se-MOS** (10 μM) fluorescence intensity changes (black bars) of individual analytes (100 μM) in comparison with those (red bars) after addition of Cys (100 μM) at 613 nm. 0. Blank; 1. Hcy; 2. GSH; 3. Ala; 4. Gln; 5. Ile; 6. Met; 7. Arg; 8. His; 9. Tyr; 10. Asp; 11. Glu; 12. Leu; 13. Gly; 14. Phe; 15. Lys; 16. Thr; 17. Ser; 18. Pro; 19. Try; 20. SO_3^{2-}; 21. $S_2O_3^{2-}$; 22. $S_2O_4^{2-}$; 23. $S_2O_5^{2-}$; 24. HSO_3^-; 25. HS^-; 26. NO·; 27. TBHP; 28. H_2O_2; 29. $^1O_2$.

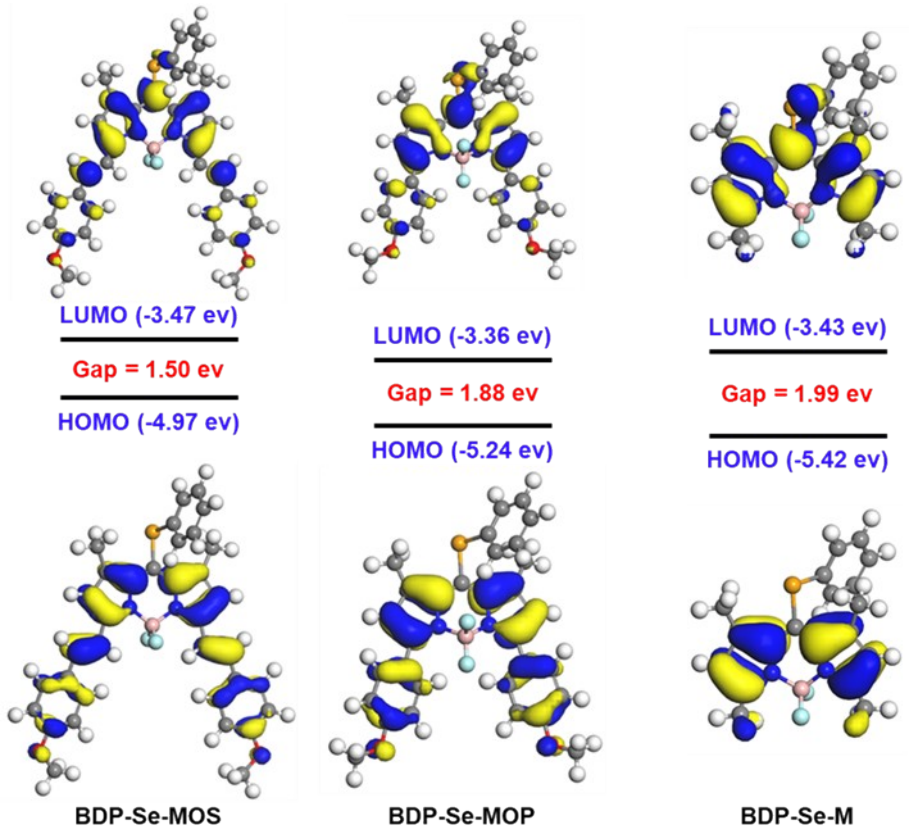

Fig. S8. Molecular orbital plots and the corresponding HOMO and LUMO energy gaps of probes.

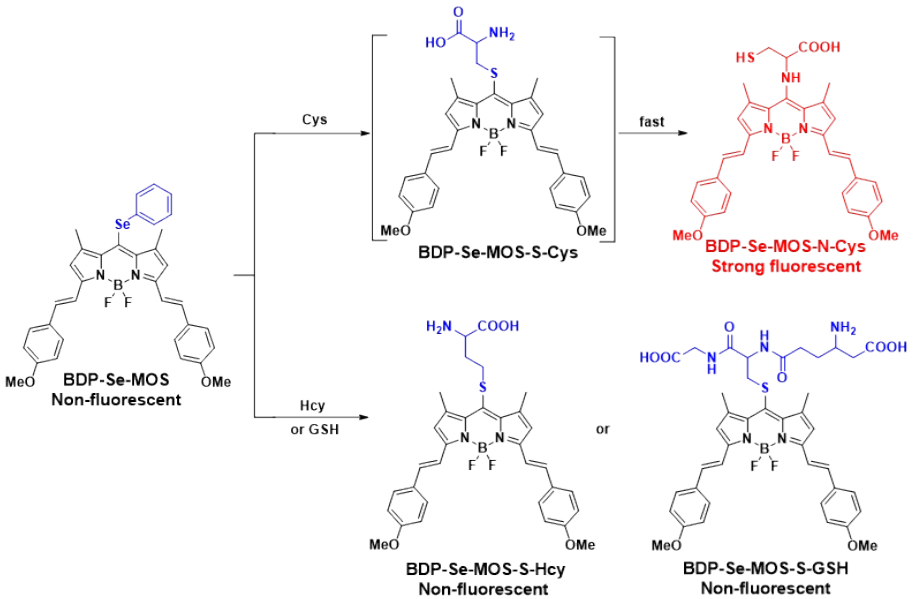

Fig. S9 Proposed reaction mechanisms of probe **BDP-Se-MOS** toward Cys, Hcy, and GSH.

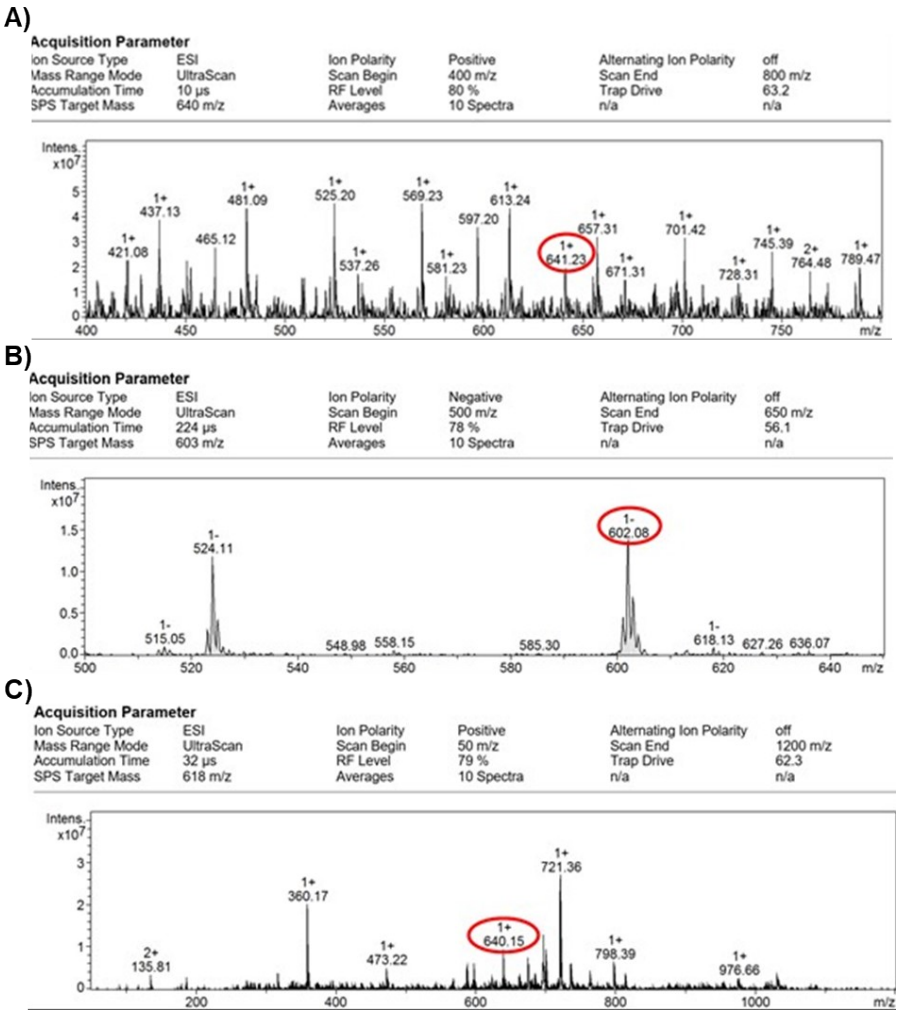

Fig. S10 The MS spectrum of (A) **BDP-Se-MOS**, (B) **BDP-Se-MOS + Cys**, (C) **BDP-Se-MOS + Hcy**.

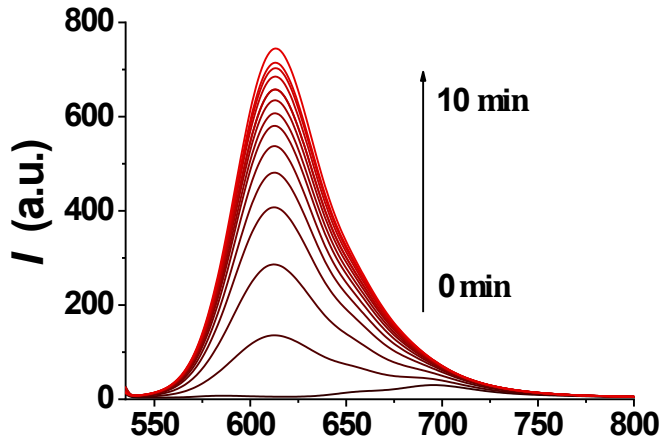

Fig. S11 Time-dependent fluorescence changes of **BDP-Se-MOS** (10 µM) activated by Cys (100 µM) Conditions: PBS buffer solutions (pH 7.4, 10 mM, containing 50% CH_3CN), 37°C, λ_{ex} = 525 nm**.**

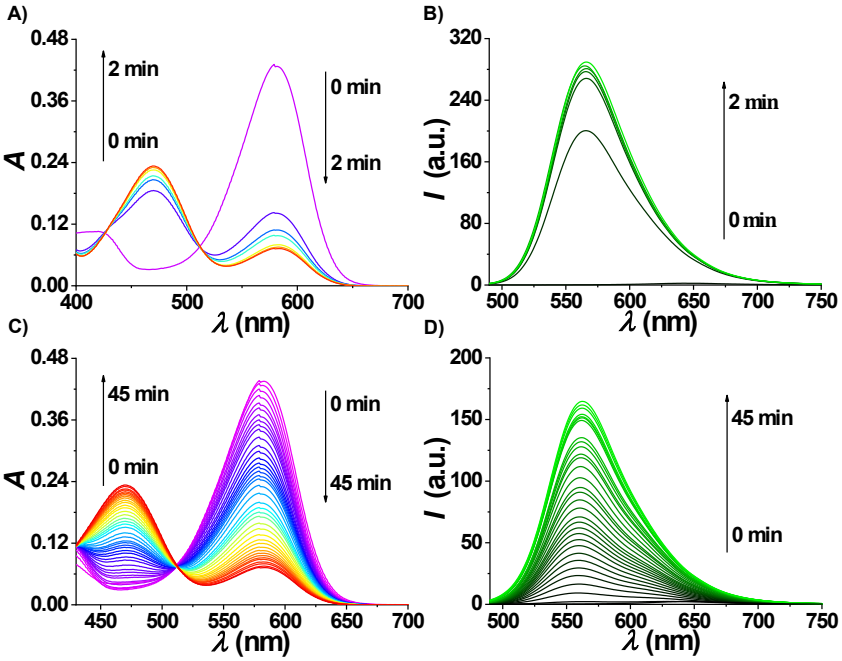

Fig. S12 Time-dependent (A, C) absorption and (B, D) emission spectral changes of **BDP-Se-MOP** (10 μM) with 10 equiv. of Cys/Hcy incubated in solution (pH 7.4, 40% CH_3CN in 10 mM PBS) at 37°C.

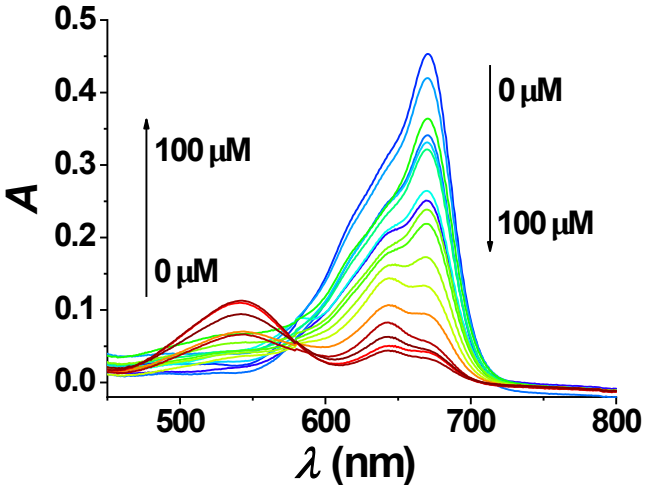

Fig. S13 Absorption spectra changes of **BDP-Se-MOS** (10 μM) incubated with increasing gradual various amounts of Cys from 0 to 100 μM in solution (pH 7.4, 50% CH_3CN in 10 mM PBS) at 37°C.

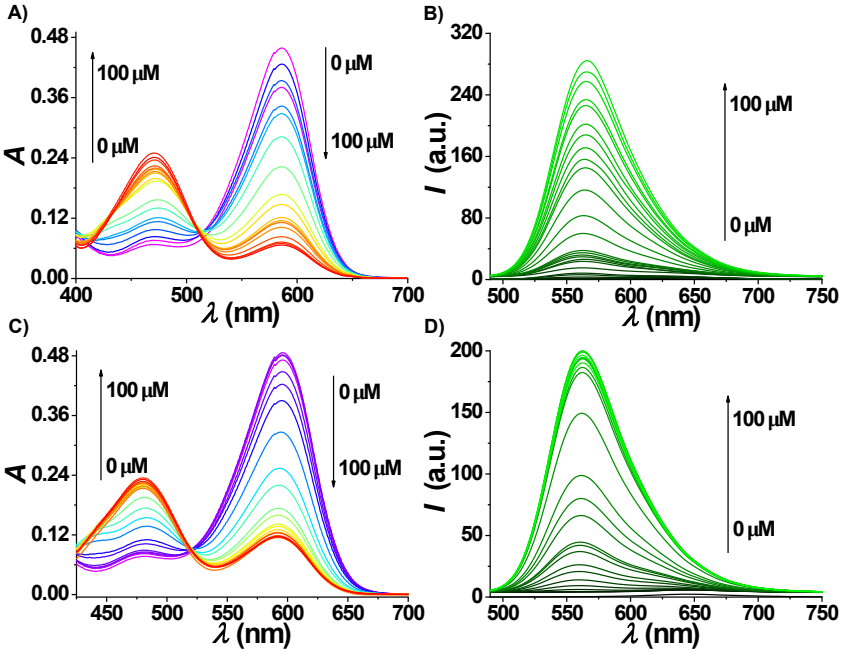

Fig. S14 Absorption (A, D) and fluorescence (B, E) spectra changes of **BDP-Se-MOP** (10 μM) incubated with increasing gradual various amounts of Cys/Hcy from 0 to 100 μM in solution (pH 7.4, 40% CH_3CN in 10 mM PBS) at 37°C.

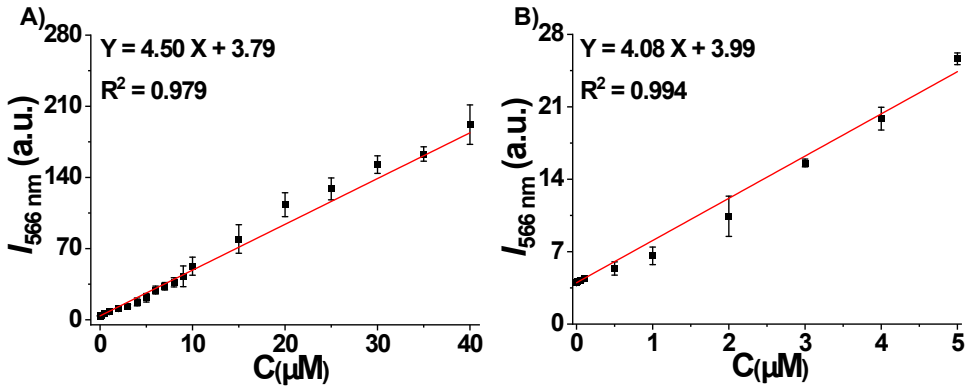

Fig. S15 A linear relationship of 566 nm fluorescence intensity (**BDP-Se-MOP**) response against (A) Cys (0–40 μM) and (B) Hcy (0–5 μM).

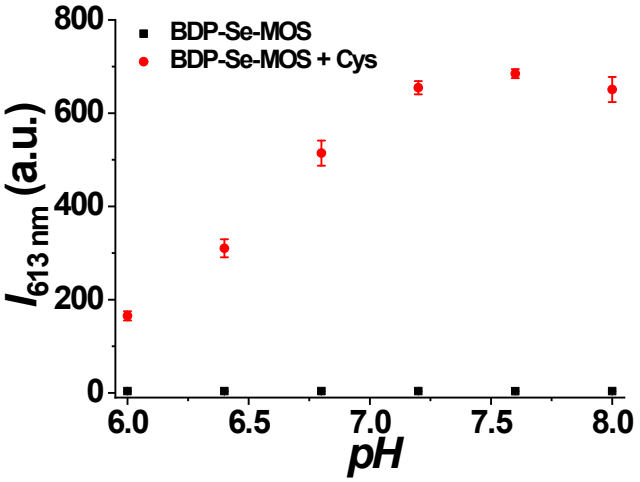

Fig. S16 The fluorescence intensity of **BDP-Se-MOS** (10 μM) absent (red circles) and present (black squares) Cys (100 μM) at different pH values. 37°C, λ_{ex} = 525 nm.

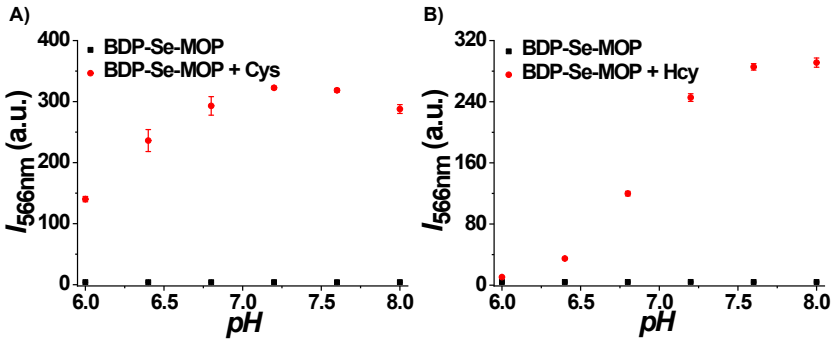

Fig. S17 The fluorescence intensity of **BDP-Se-MOP** (10 μM) absent (red circles) and present (black squares) (A) Cys, (B) Hcy (100 μM) at different pH values. 37°C, λ_{ex} = 456 nm.

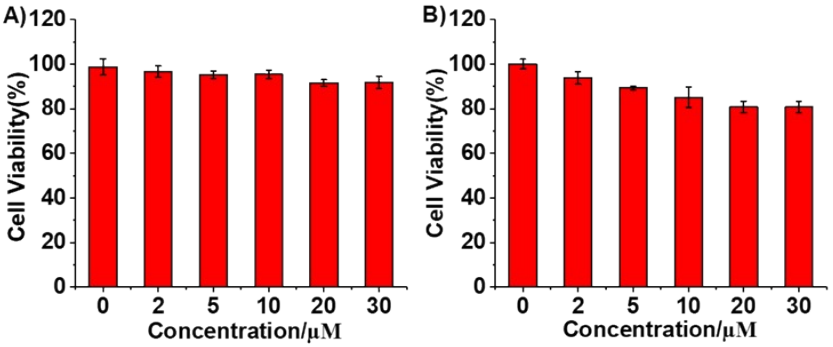

Fig. S18 Cell viability assay of **BDP-Se-MOS** in (A) HepG2 cells and (B) QSG-7701 cells, all compounds were incubated with the cells for 24 h, and the cells viability was observed *via* MTT assays.

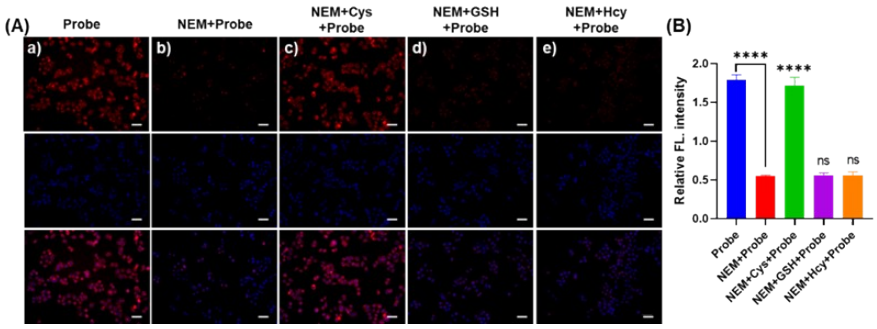

Fig. S19 (A) Fluorescence imaging of intracellular and exogenous Cys by **BDP-Se-MOS**. (a): the cells were cultured with **BDP-Se-MOS** (10 μM) for 2 h. (b): the cells were pre-cultured with NEM (1 mM) for 1 h and then cultured with **BDP-Se-MOS** (10 μM) for 2 h. (c, d, e): the cells were pre-cultured with NEM (1 mM) for 1 h, cultured with Cys, Hcy or GSH (200 μM) for 40 min, then incubated with **BDP-Se-MOS** (10 μM) for 2 h. (B) Fluorescence intensities of (A). Statistical analysis was performed with a two-tailed Student's t-test. **** $P < 0.0001$, n.s. denotes no significant difference. Blue channel: the cells were stained with Hoechst 33342 (1 $\mu g \cdot mL^{-1}$), λ_{ex} = 400 nm, λ_{em} = 435–485 nm. Red channel: λ_{ex} = 560 nm, λ_{em} = 565–605 nm. Scale bar: 50 μm.

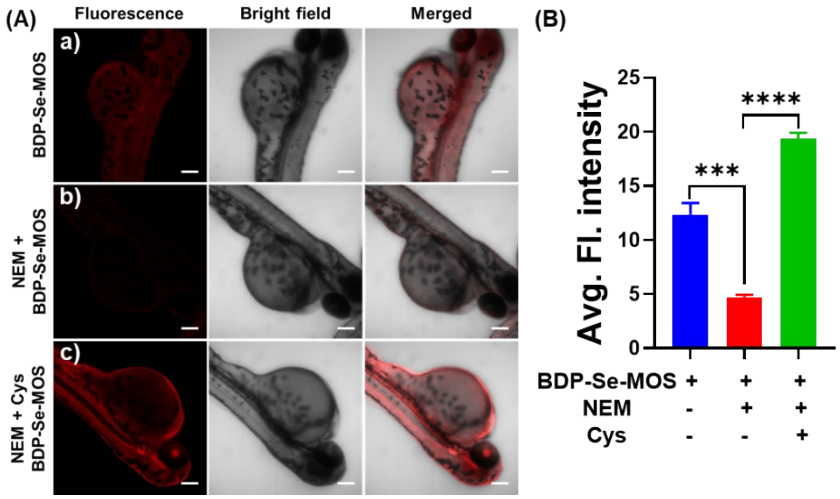

Fig. S20. (A) Fluorescent images of **BDP-Se-MOS** in zebrafish. (a) **BDP-Se-MOS** (10 μM) was incubated for 1 h; (b) pretreat the zebrafish with NEM (1 mM) for 30 min and incubate with **BDP-Se-MOS** for 1 h; (c) zebrafish was pre-treated with NEM for 30 min, then Cys (200 μM) was added for 30 min and finally **BDP-Se-MOS** was incubated for 1 h. (D) The fluorescence intensity of (A). Statistical analysis was performed with a two-tailed Student's t-test. ***$p < 0.001$, **** $P < 0.0001$. λ_{ex} = 530–570 nm, λ_{em} = 575–640 nm. Scale bar: 100 μm.

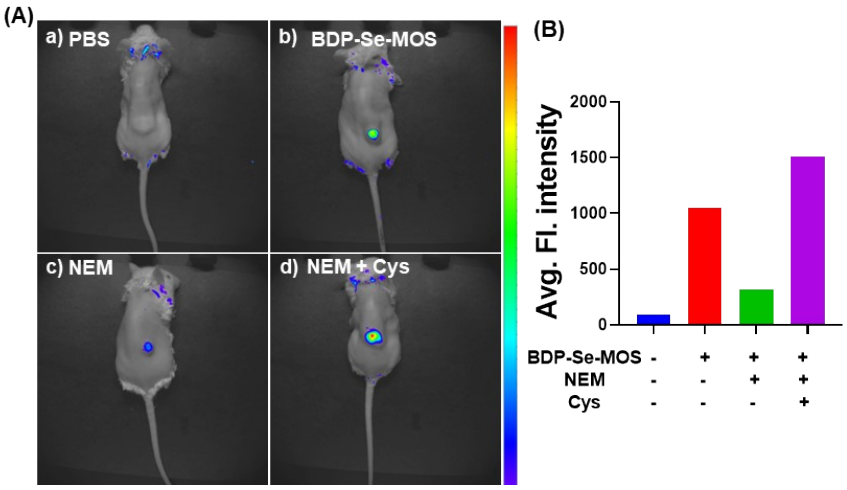

Fig. S21 (A) Fluorescent images of probe **BDP-Se-MOS** in Kunming mice. (a) PBS was incubated for 1 h; (b) **BDP-Se-MOS** was incubated for 1 h; (c) pretreat the mice with 500 μM NEM for 30 min and incubate with **BDP-Se-MOS** for 1 h; (d) the mice were pre-treated with 500 μM NEM for 30 min, then 100 μM Cys was added for 30 min and finally **BDP-Se-MOS** was incubated for 1 h. (B) The fluorescence intensity of A. λ_{ex} = 540–580 nm, λ_{em} = 590–670 nm.

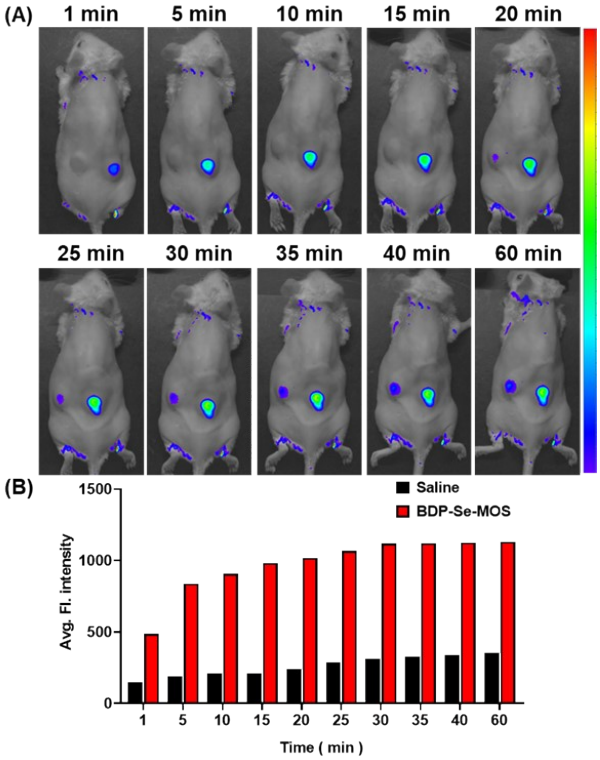

Fig. S22 *In vivo* fluorescence imaging performance of **BDP-Se-MOS** in living Kunming mice. (A)The mice were given subcutaneous injection of **BDP-Se-MOS**. After incubation, images were taken at time 1, 5, 10, 15, 20, 25, 30, 35, 40 and 60 min, respectively; (B) Averaged intensity of the images (A). λ_{ex} = 540–580 nm, λ_{em} = 590–670 nm.

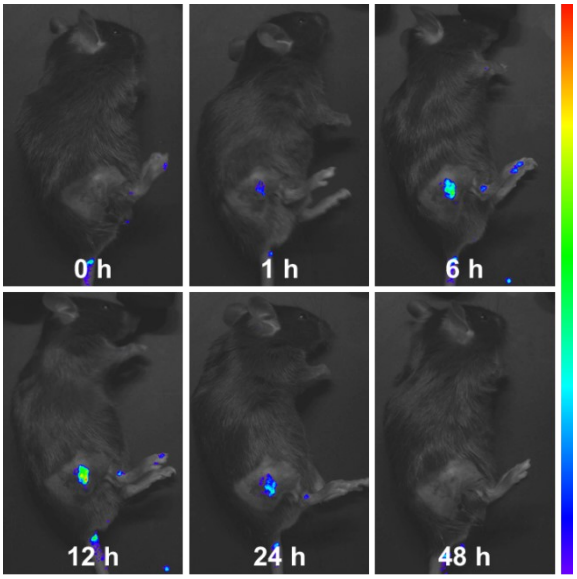

Fig. S23 Fluorescence images at different times of tumor mice were harvested after tail vein injection of **BDP-Se-MOS** (1 mg/kg). λ_{ex} = 540–580 nm, λ_{em} = 590–670 nm.

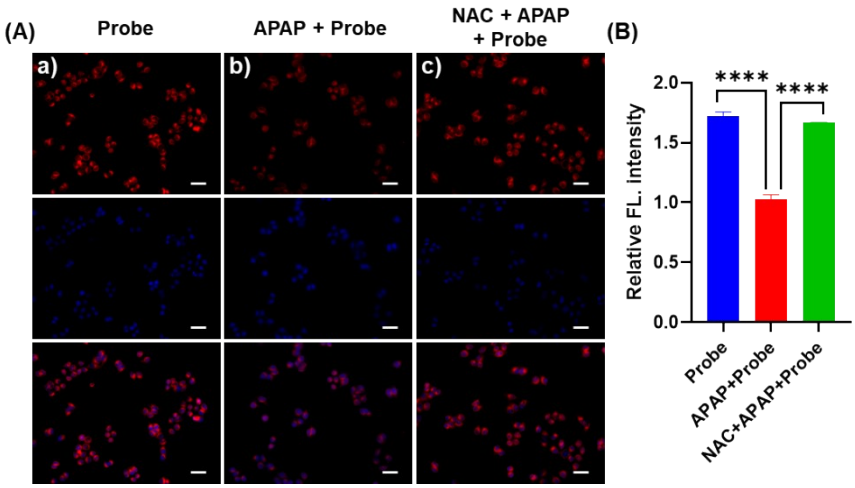

Fig. S24 (A) Fluorescence imaging of APAP-induced liver injury in HepG2 cells. (a) the cells were only incubated with **BDP-Se-MOS** (10 μM) for 2 h. (b) the cells were loaded with **BDP-Se-MOS** (10 μM) for another 2 h after preincubation with APAP (500 μM) for 8 h. (c) the cells were treated with **BDP-Se-MOS** (10 μM) for 2 h after preincubation with NAC (500 μM) for 1 h and preincubation with APAP (500 μM) for 8 h. (B) Fluorescence intensity of (A). Statistical analysis was performed with a two-tailed Student's t-test. ****$p < 0.0001$. Blue channel: the cells were stained with Hoechst 33342 (1 μg·mL^{-1}), λ_{ex} = 400 nm, λ_{em} = 435–485 nm. Red channel: λ_{ex} = 560 nm, λ_{em} = 565–605 nm. Scale bar: 50 μm.

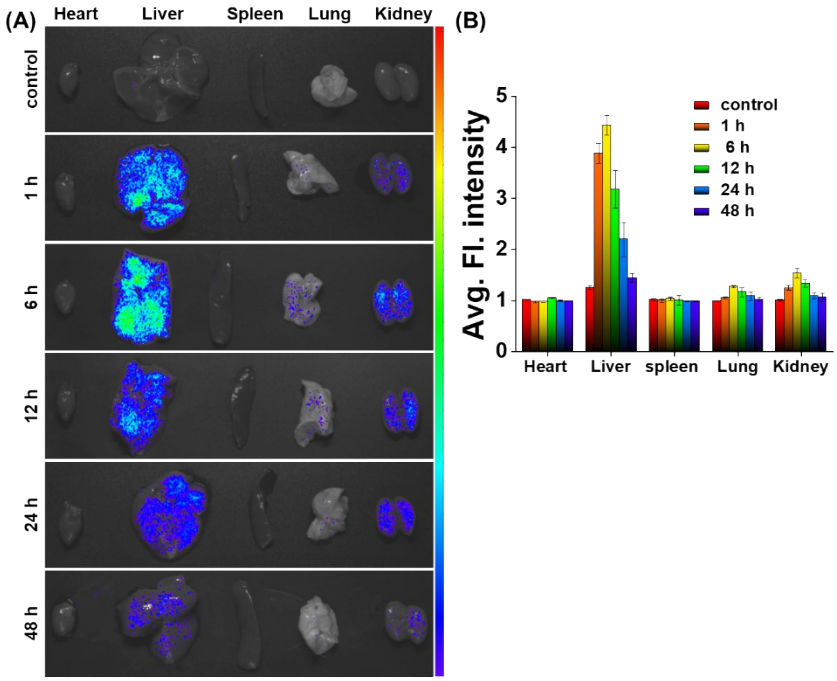

Fig. S25 *In vivo* distribution and clearance behaviors of **BDP-Se-MOS** (1mg/kg). (A) Fluorescence images of major organs from Kunming mice at different times; (B) The corresponding fluorescence intensity values of major organs. From left to right: heart, liver, spleen, lung and kidney. λ_{ex} = 540–580 nm, λ_{em} = 590–670 nm.

4. NMR spectra

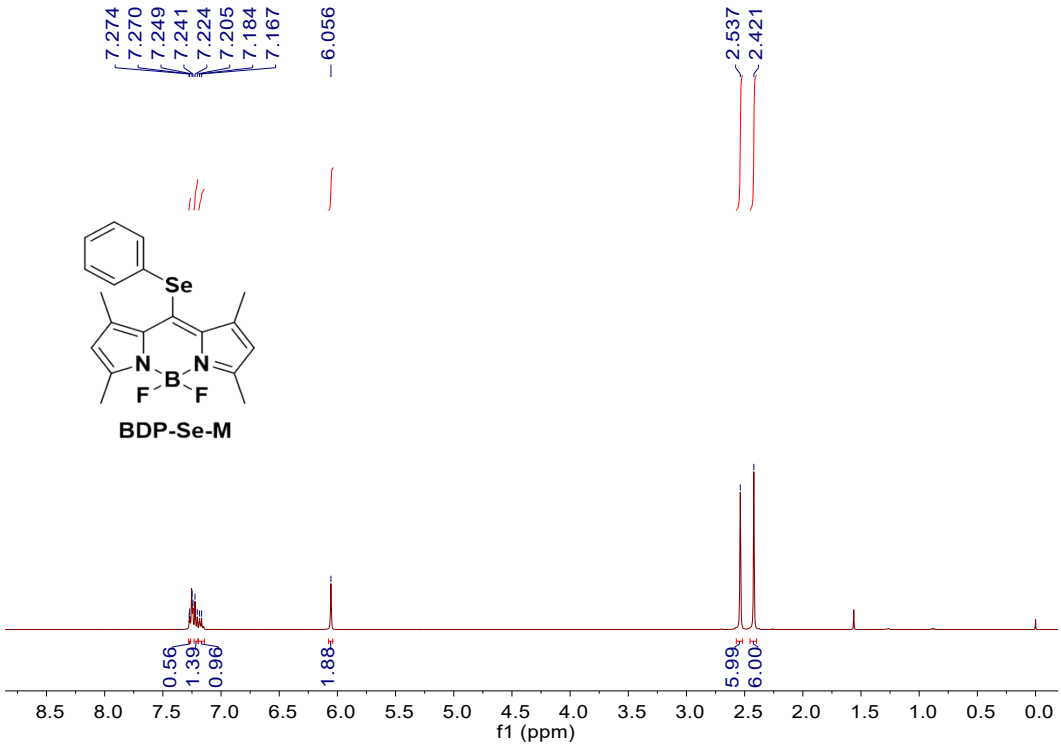

Fig. S26 ^{1}H NMR spectra of **BDP-Se-M** in $CDCl_3$.

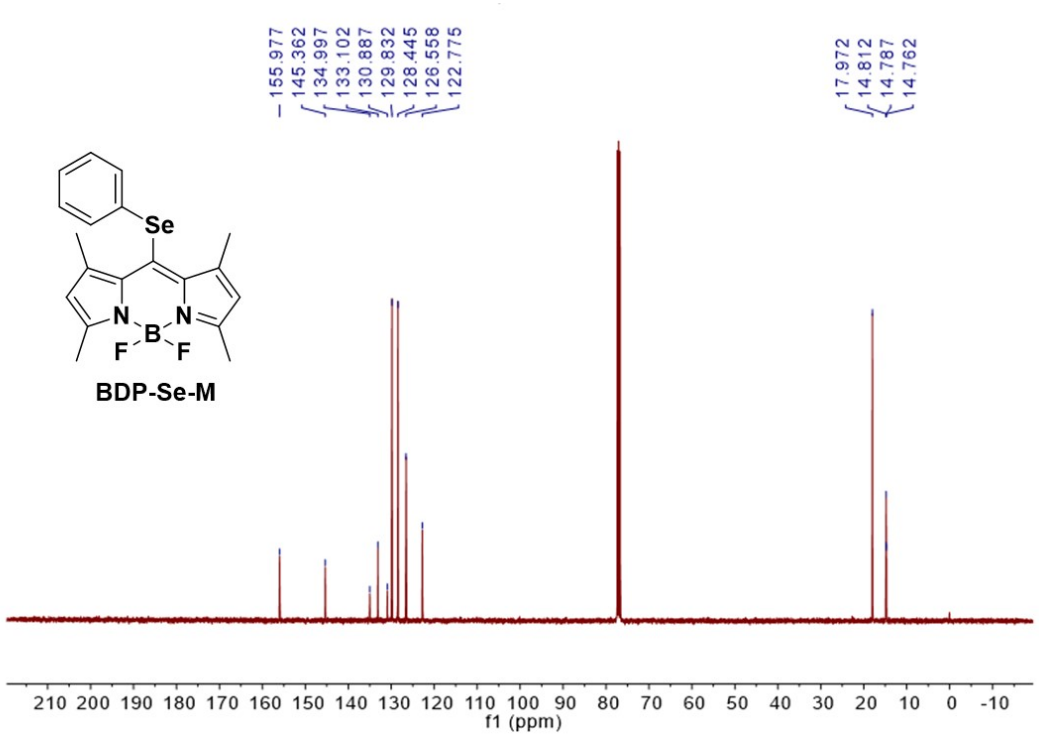

Fig. S27 ^{13}C NMR spectra of **BDP-Se-M** in $CDCl_3$.

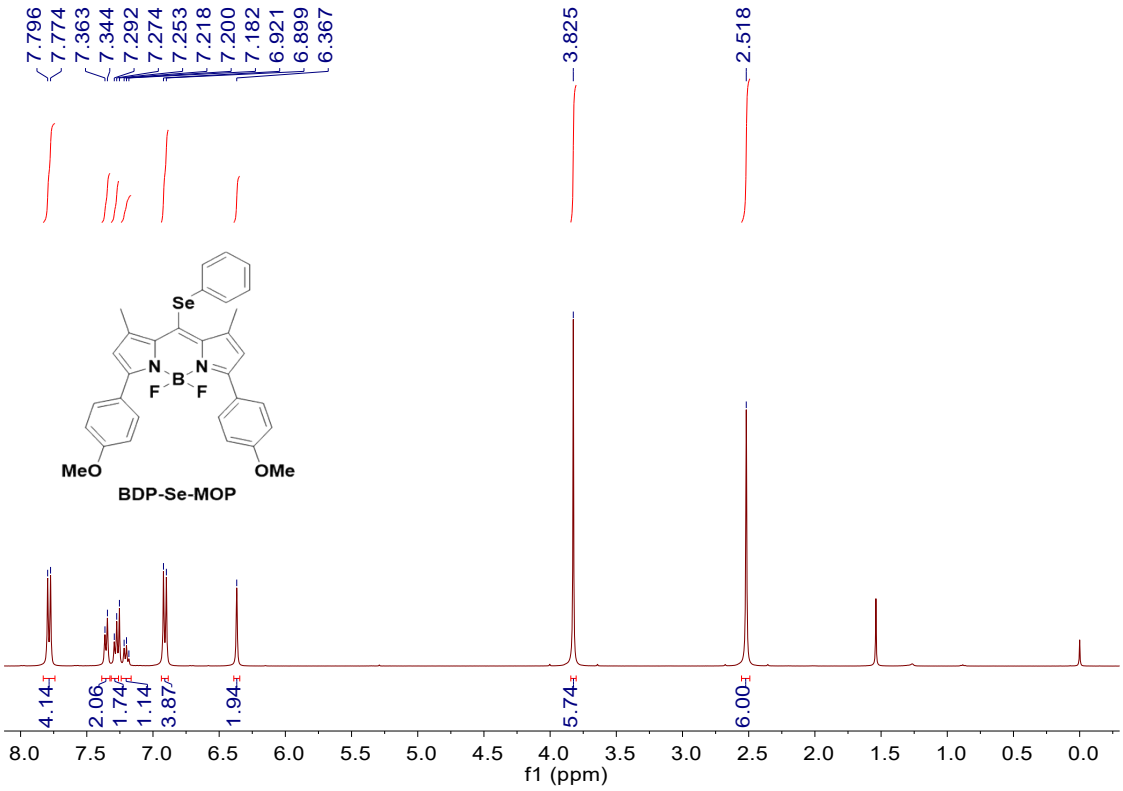

Fig. S28 ^{1}H NMR spectra of **BDP-Se-MOP** in $CDCl_3$.

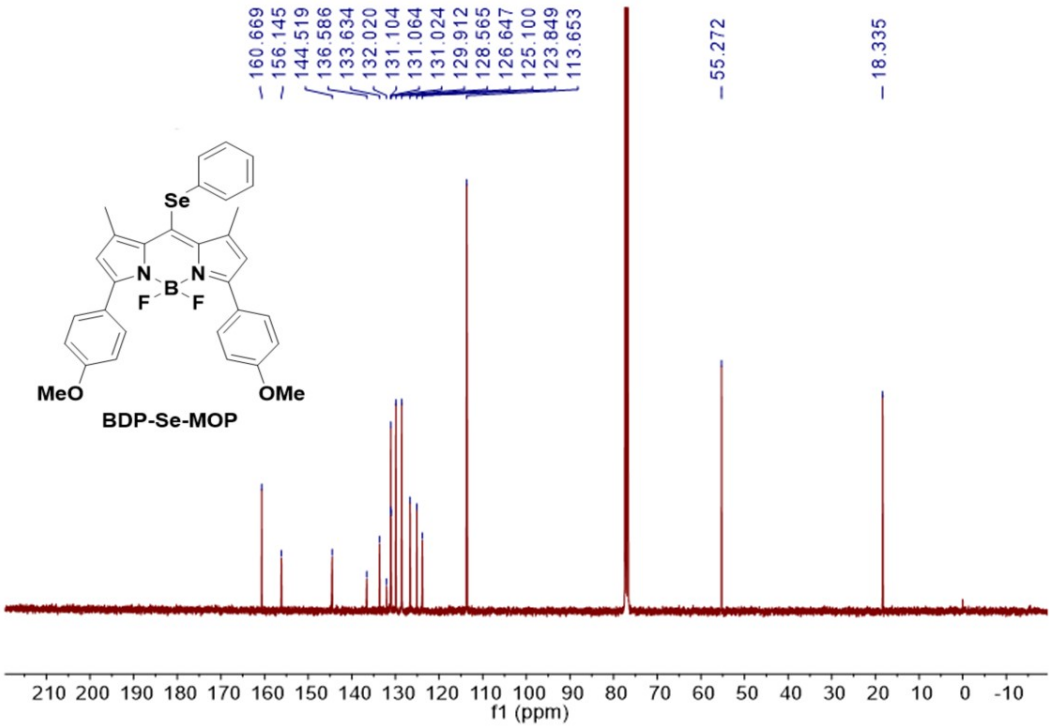

Fig. S29 ^{13}C NMR spectra of **BDP-Se-MOP** in $CDCl_3$.

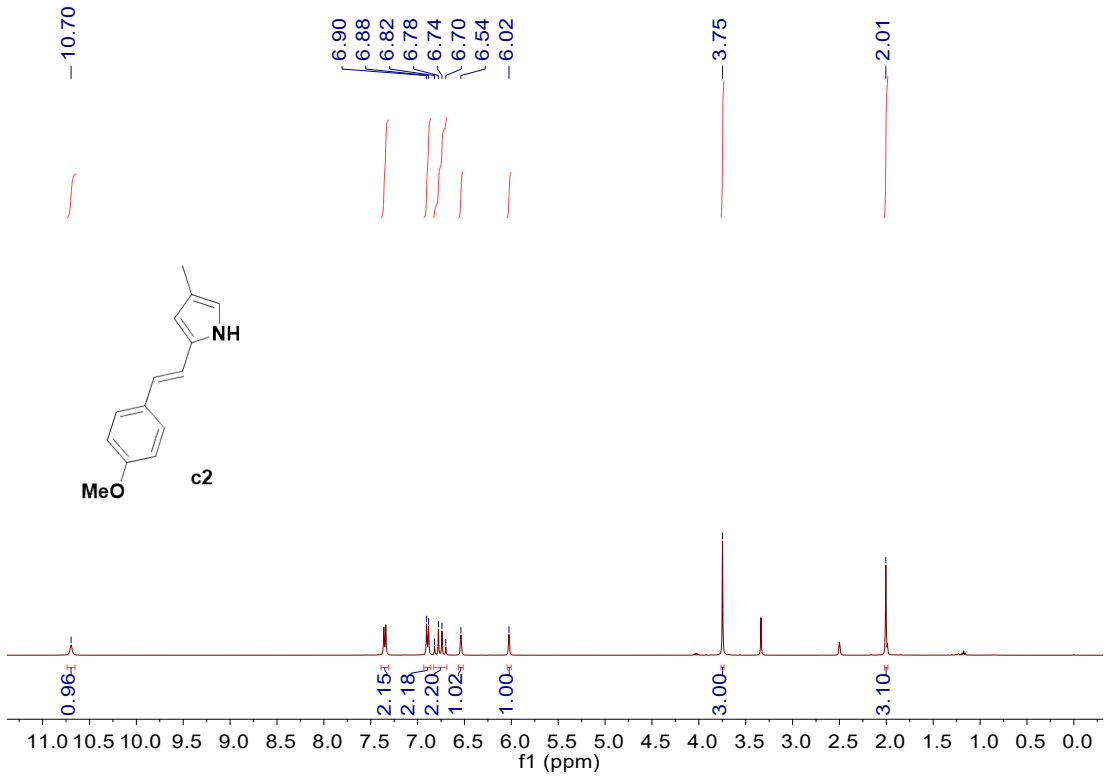

Fig. S30 ^{1}H NMR spectra of **c2** in DMSO.

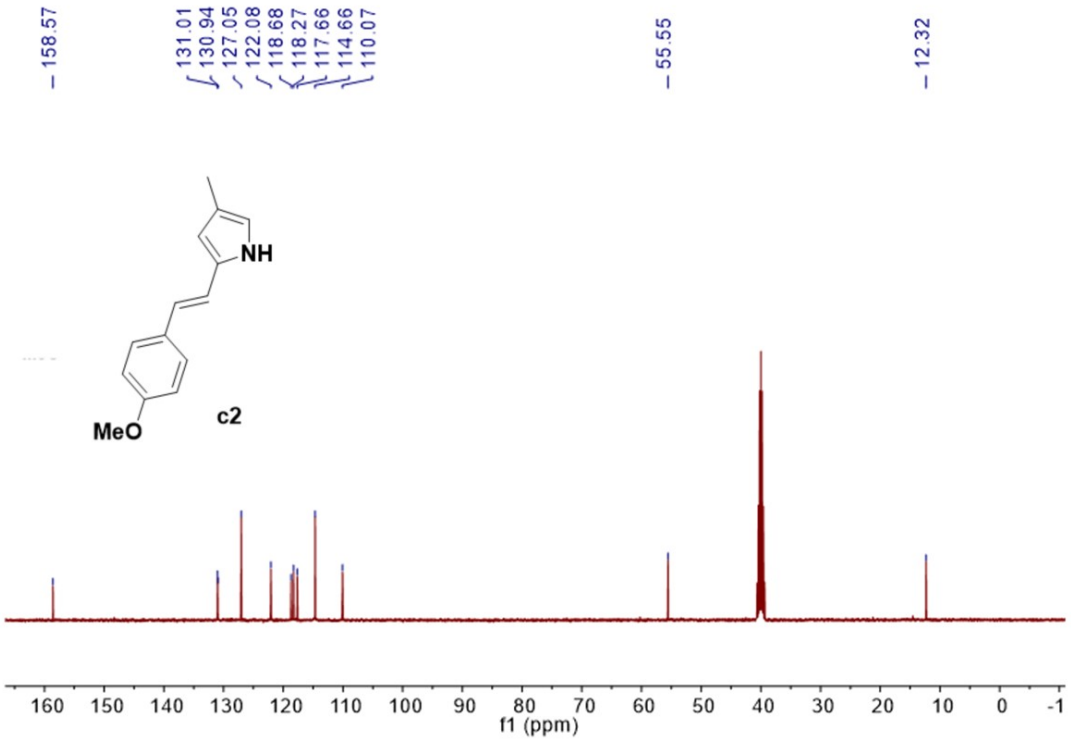

Fig. S31 ^{13}C NMR spectra of **c2** in DMSO.

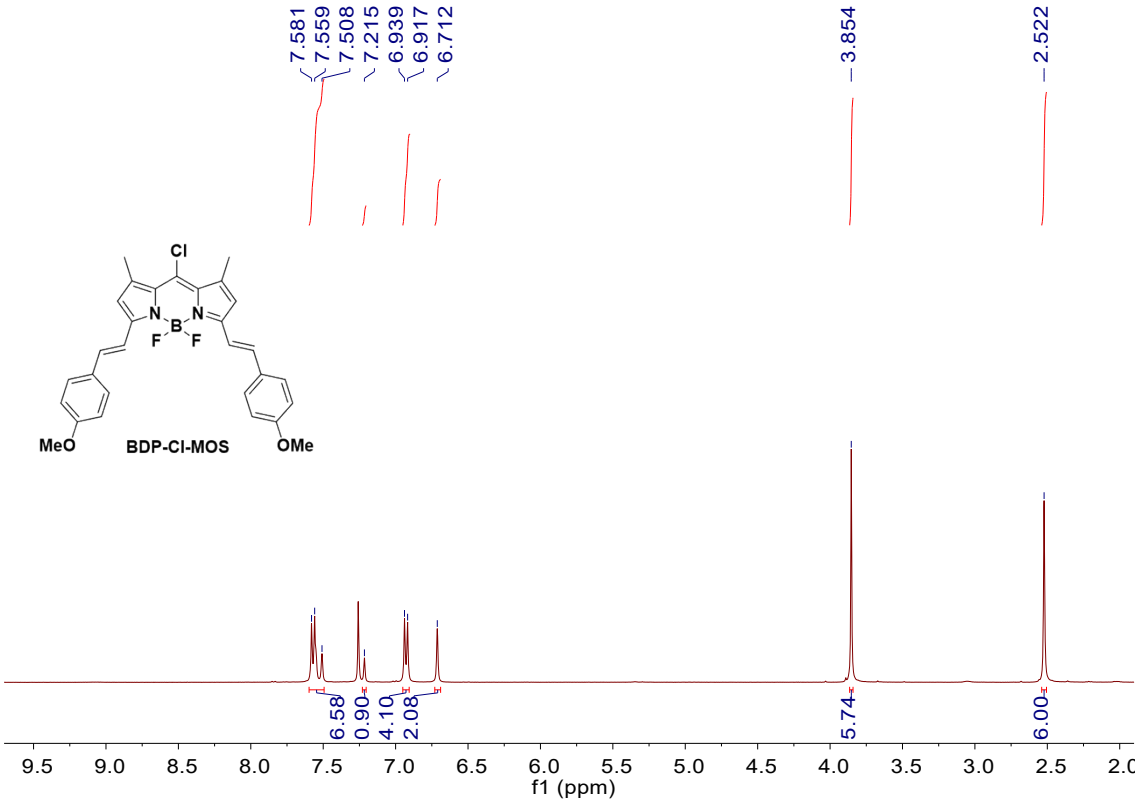

Fig. S32 ^{1}H NMR spectra of **BDP-Cl-MOS** in $CDCl_3$.

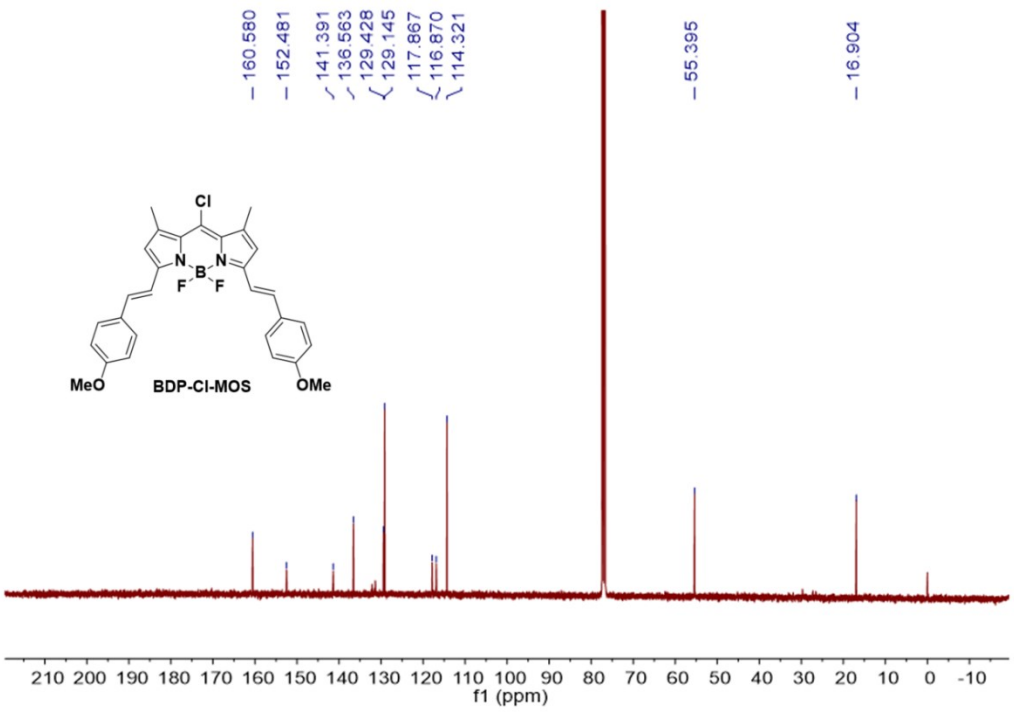

Fig. S33 ^{13}C NMR spectra of **BDP-Cl-MOS** in $CDCl_3$.

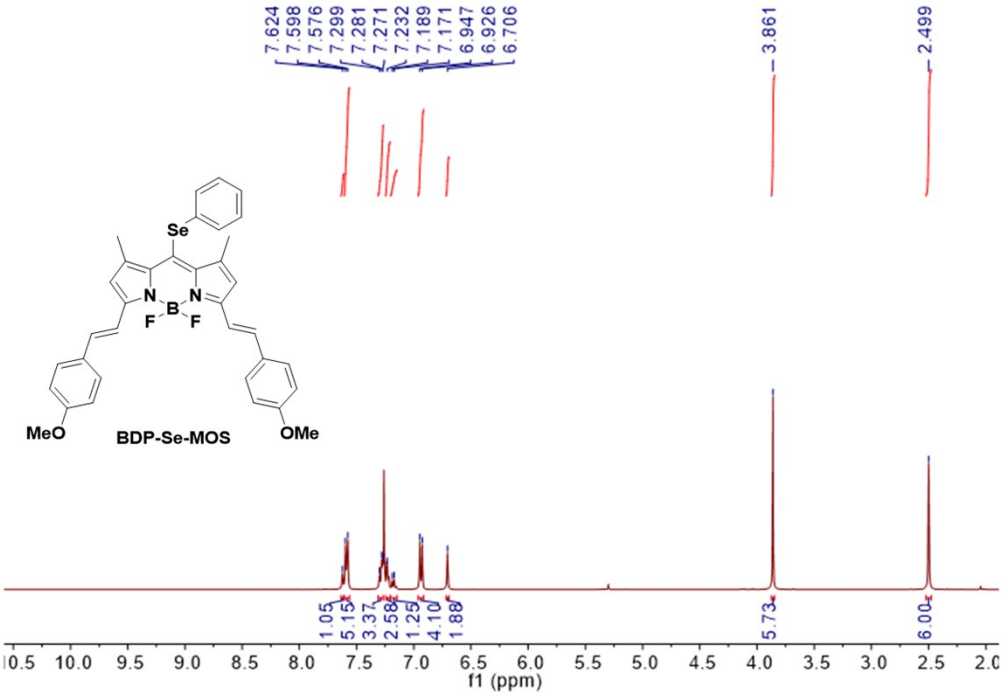

Fig. S34 ^{1}H NMR spectra of **BDP-Se-MOS** in $CDCl_3$.

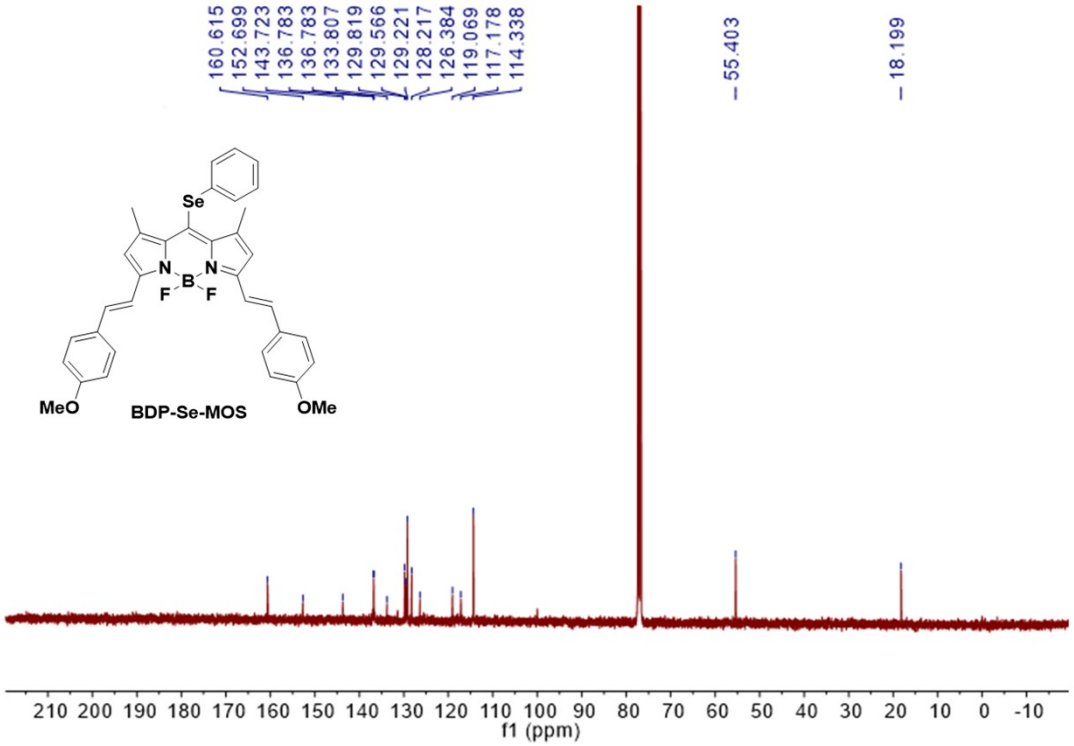

Fig. S35 ^{13}C NMR spectra of **BDP-Se-MOS** in $CDCl_3$.

5. References

1. J. Zhang, X. Ji, H. Ren, J. Zhou, Z. Chen, X. Dong, W. Zhao, *Sensor. Actuat. B-Chem*., 2018, **260**, 861–869.
2. J. Gao, Y. Tao, J. Zhang, N. Wang, X. Ji, J. He, Y. Si, W. Zhao, *Chem. Eur. J*., 2019, **25**, 11246–11256.